Contract No:

This document was prepared in conjunction with work accomplished under Contract No. DE-AC09-08SR22470 with the U.S. Department of Energy (DOE) Office of Environmental Management (EM).

We put science to work.™

Savannah River National Laboratory™

OPERATED BY SAVANNAH RIVER NUCLEAR SOLUTIONS

A U.S. DEPARTMENT OF ENERGY NATIONAL LABORATORY • SAVANNAH RIVER SITE • AIKEN, SC

Updated Groundwater Flow Simulations of the Savannah River Site General Separations Area

G. P. Flach

January 15, 2019

SRNL-STI-2018-00643, Revision 0

SRNL.DOE.GOV

DISCLAIMER

Printed in the United States of America

Prepared for
U.S. Department of Energy

Keywords: *Performance Assessment, PORFLOW, PEST*

Retention: *Permanent*

Updated Groundwater Flow Simulations of the Savannah River Site General Separations Area

G. P. Flach

January 15, 2019

Prepared for the U.S. Department of Energy under contract number DE-AC09-08SR22470.

Savannah River National Laboratory™

OPERATED BY SAVANNAH RIVER NUCLEAR SOLUTIONS

REVIEWS AND APPROVALS

AUTHORS:

G. P. Flach, SRR Closure & Disposal Assessment Date

TECHNICAL REVIEW:

S. E. Aleman, Threat Assessments, Reviewed per E7 2.60 Date

APPROVAL:

D. A. Crowley, Manager Date
Environmental Modeling

L. T. Reid, Manager Date
Environmental Restoration Technologies

K. H. Rosenberger, Manager Date
Closure & Disposal Assessment

EXECUTIVE SUMMARY

The groundwater flow model supporting Performance Assessments (PAs) and Composite Analyses (CAs) at the Savannah River Site was significantly revised in 2016 and 2017 using new hydrostratigraphic surfaces, updated well water level calibration targets, and semi-automated model calibration with the PEST optimization code. This model is referred to as “GSA_2016”. This report documents further refinement of the GSA_2016 model in 2018 to incorporate updates to model calibration targets, closure of the H-Area Ash Basin, construction of E-Area Slit Trench operational covers, and plume information from the Mixed Waste Management Facility and Low-Level Radioactive Waste Disposal Facility. Another objective was to lower hydraulic head residuals by adding another calibration zone. The resulting model is referred to as “GSA_2018”.

TABLE OF CONTENTS

LIST OF TABLES vii
LIST OF FIGURES vii
LIST OF ABBREVIATIONS ix
1.0 Introduction 1
2.0 Updated information 1
3.0 Model recalibration 4
4.0 Groundwater flow simulation results 9
4.1 PEST calibration 9
4.2 Simulation validation 11
4.3 Simulation results 15
4.4 Simulation uncertainty 20
4.5 Comparison to GSA_2016 model 20
5.0 References 25

LIST OF TABLES

Table 4-1. Hydraulic head residual statistics. 9

Table 4-2. Stream baseflow validation targets. 9

Table 4-3. Hydraulic conductivity summary for the GSA_2018.LW model. 11

Table 4-4. Global mass balance (ft^3/s). 12

Table 4-5. Aquifer zone mass balances (ft^3/s). 12

Table 4-6. Boundary condition mass balances (ft^3/s). 13

Table 4-7. Parameter confidence limits. 20

LIST OF FIGURES

Figure 2-1. Annotated aerial photo showing the former H-Area Ash Basin and E-Area Slit Trench operational covers. 2

Figure 2-2. Cone Penetration Testing (CPT) locations 01 through 10 near E-Area and water table contours. 3

Figure 2-3. Cone Penetration Testing (CPT) data near E-Area and plumes conceptual model. 3

Figure 3-1. Conductivity zone “FHbasins2” added to GSA_2018 calibration. 4

Figure 3-2. Simulated groundwater pathlines for GSA_2016 model prior to placement of low-infiltration covers. 5

Figure 3-3. Simulated groundwater pathlines for GSA_2016 model after placement of low-infiltration covers. 6

Figure 3-4. Simulated groundwater pathlines for GSA_2018 model prior to placement of low-infiltration covers. 7

Figure 3-5. Simulated groundwater pathlines for GSA_2018 model after placement of low-infiltration covers. 8

Figure 4-1. Hydraulic head residuals and water table surface for the GSA_2018.LW model. 10

Figure 4-2. Simulated seepage faces compared to surveyed seeplines. 13

Figure 4-3. Hydraulic head crossplots. 14

Figure 4-4. Simulated water table (ft). 16

Figure 4-5. Kriging interpolation representation of water table measurements (ft). 16

Figure 4-6. Simulated hydraulic head in the Upper Aquifer Zone (ft). 17

Figure 4-7. Simulated hydraulic head in the Lower Aquifer Zone (ft). 17

Figure 4-8. Simulated hydraulic head in the Gordon Aquifer Unit (ft). 18

Figure 4-9. Kriging interpolation representation of Gordon aquifer unit (GAU) measurements (ft). 18

Figure 4-10. Simulated surface flux (ft/d). 19

Figure 4-11. Particle tracking results for GSA2016.LW model. 21

Figure 4-12. Particle tracking results for GSA2018.LW model. 21

Figure 4-12. Plan view of 1Q17 Tc-99 plume near SDU4 22

Figure 4-12. Simulated groundwater particle tracks and head contours near Saltstone Disposal Unit 4 and well ZBG-2 based on the GSA_2016.LW model. 23

LIST OF ABBREVIATIONS

AAA	A and AA horizons
CA	Composite Analysis
CPT	Cone Penetration Testing
GAU	Gordan aquifer unit
GCU	Gordon confining unit
GSA	General Separations Area
LAZ	Lower UTR aquifer zone
LLRWDF	Low-Level Radioactive Waste Disposal Facility
MWMF	Mixed Waste Management Facility
PA	Performance Assessment
SRNL	Savannah River National Laboratory
TCCZ	Tan Clay confining zone
TZ	Transmissive zone
UAZ	Upper UTR aquifer zone
UTR	Upper Three Runs
VOC	volatile organic compound

This page intentional left blank

1.0 Introduction

The groundwater flow model supporting Performance Assessments (PAs) and Composite Analyses (CAs) at the Savannah River Site was significantly revised in 2016 and 2017 (Flach et al. 2017a, b) using new hydrostratigraphic surfaces (Bagwell et al. 2017), updated well water level calibration targets (Hiergesell et al. 2015), and semi-automated model calibration with the PEST optimization code (Flach 2015). This model is referred to as "GSA_2016".

This report documents further refinement of the GSA_2016 model in 2018 to incorporate updates to model calibration targets, closure of the H-Area Ash Basin, construction of E-Area Slit Trench operational covers, and plume information from the Mixed Waste Management Facility (MWMF) and Low-Level Radioactive Waste Disposal Facility (LLRWDF). Another objective was to lower hydraulic head residuals by adding another calibration zone. The resulting model is referred to as "GSA_2018".

2.0 Updated information

The GSA_2016 model was calibrated to well water levels from the period 2004 to 2014 (Hiergesell et al. 2015). Wohlwend (2018) extended the data averaging period from 2004-August 2014 to 2004-March 2018. The number of calibration targets increased from 638 to 711. Near Z-Area, the number of target well locations increased from 3 in the upper aquifer zone and 7 in the lower aquifer zone to 6 and 11, respectively.

As seen in the 2018 aerial photo in Figure 2-1, the H-Area Ash Basin is no longer in service, and thus not a source of enhanced infiltration in the groundwater flow model. Conversely, operational covers over closed Slit Trenches in E-Area reduce local infiltration. These changes in the field correspond to boundary condition changes in the flow model.

Multiple depth Cone Penetration Testing (CPT) at 10 locations near E-Area shown in Figure 2-2 has delineated tritium (H-3) and volatile organic compound (VOC) plumes presumed to emanate from the MWMF/LLRWDF and E-Area (Kubilius and Joyce 2018). Figure 2-3 list species concentrations as a function of depth and elevation. Intervals of elevated concentration are highlighted with darker shading. The conceptual model, also depicted in Figure 2-3, is that deeper, mixed H-3 and VOC, plumes originate from the MWMF while shallower, H-3 only, plumes are associated with E-Area. Simulated groundwater pathlines can be compared to the MWMF plume information to calibrate and/or validate the flow model.

Figure 2-1. Annotated aerial photo showing the former H-Area Ash Basin and E-Area Slit Trench operational covers.

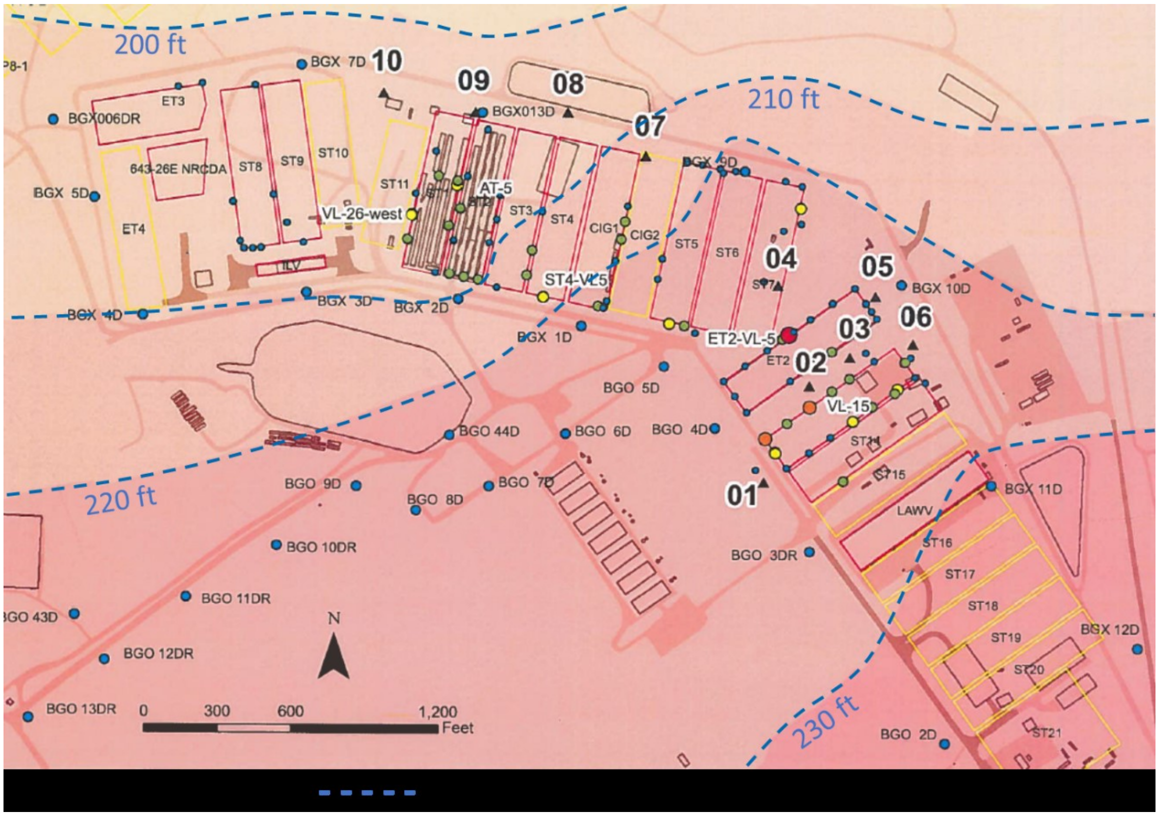

Figure 2-2. Cone Penetration Testing (CPT) locations 01 through 10 near E-Area and water table contours.

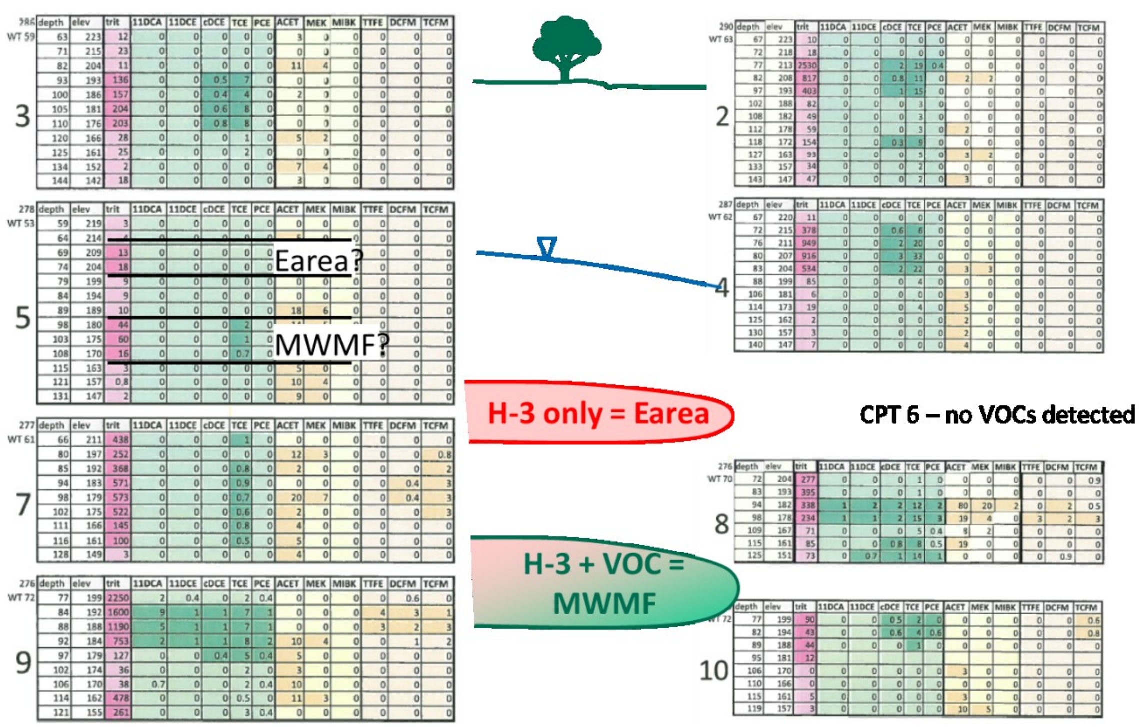

Figure 2-3. Cone Penetration Testing (CPT) data near E-Area and plumes conceptual model.

3.0 Model recalibration

Hydraulic head residuals (simulated hydraulic head minus measured head) were observed to be biased low around the F- and H-Area seepage basins (Flach et al 2017b Figure 7-6) in the GSA_2016 model. To enable better agreement with the field data, Solid Waste Programs proposed model recalibration with one or more conductivity zones in addition to "Harea" and "Zarea2" (Flach et al 2017b Figure 6-30). After several iterations using different polygons, the "FHBasins2" geometry shown in Figure 3-1 was selected for GSA_2018 recalibration.

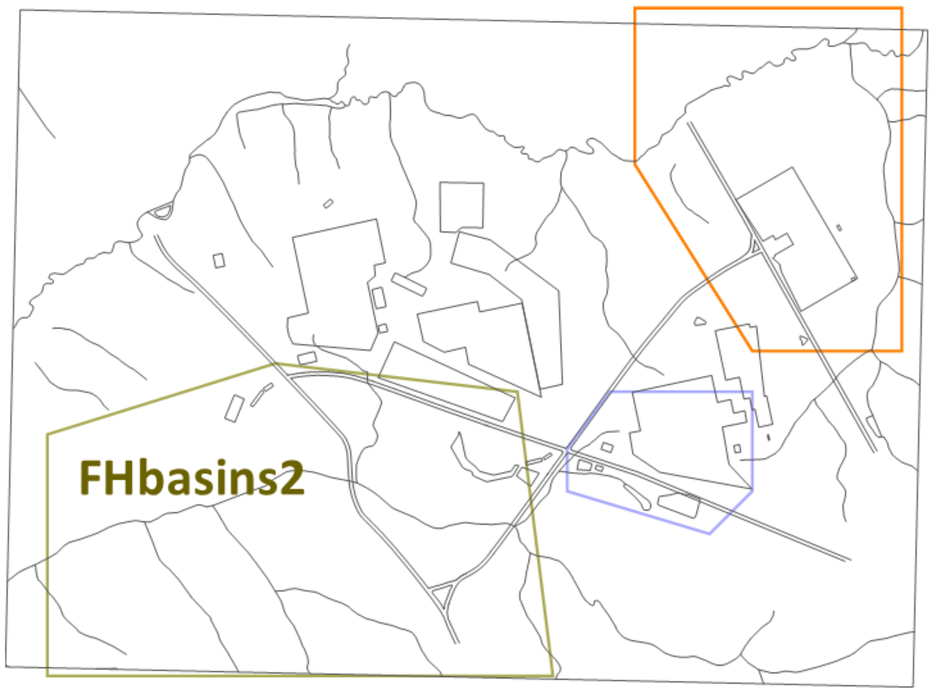

Figure 3-1. Conductivity zone "FHbasins2" added to GSA_2018 calibration.

Only the previously recommended GSA_2016.LW model (Flach et al 2017b Section 7.5) was recalibrated, where "LW" refers to a Layer-Cake conductivity field and Weighted optimization. Like previous calibration efforts, variations in Gordon confining unit (GCU) conductivity were handled outside the PEST code through parametric study, while conductivities in higher hydrostratigraphic units were adjusted within PEST. The GSA_2016 model assumed a GCU vertical conductivity of 7.5e-5 ft/day. The GSA_2018 model assumes 1.0e-5 ft/day to achieve a better match to groundwater pathlines inferred from MWMF plume data.

Figure 3-2 through Figure 3-5 illustrate simulated pathlines for the GSA_2016 and GSA_2018 models with and without low-infiltration covers over MWMF, LLRWDF and the nearby Old Burial Ground. Early plume migration from the MWMF occurred before placement of these covers, while more recent travel reflects these surface features. Particle tracking was performed in reverse from the top and bottom of the sample intervals and locations shown in Figure 2-2 that exhibit elevated H-3 and elevated VOC concentrations. Backward particle tracks using the GSA_2016 flow field generally surface short of the MWMF / LLRWDF disposal area, whereas reverse pathlines from the GSA_2018 flow field generally terminate within the MWMF / LLRWDF footprint, particularly prior to capping. On this basis, a GCU vertical conductivity of 1.0e-5 ft/day was adopted for the GSA_2018 model.

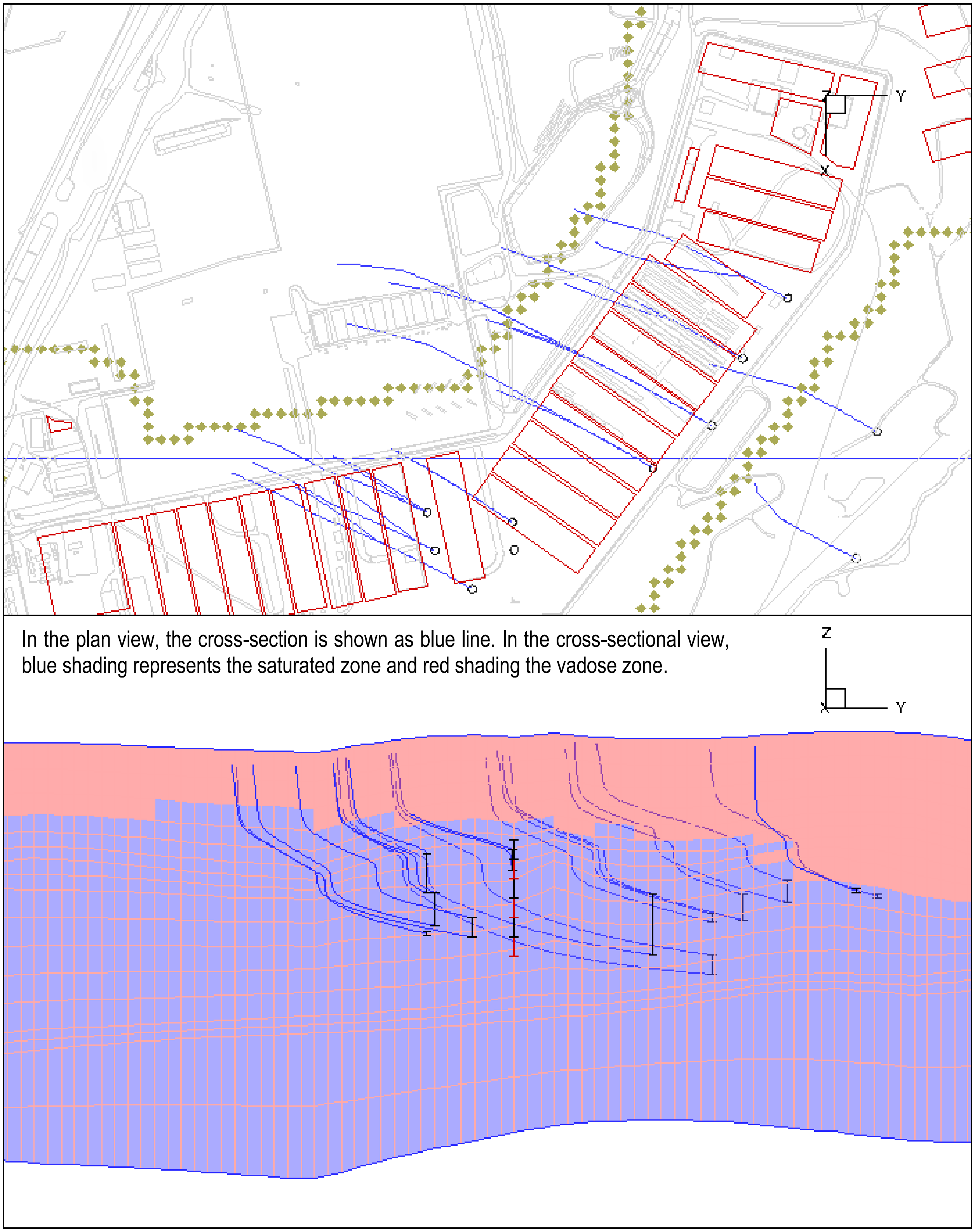

Figure 3-2. Simulated groundwater pathlines for GSA_2016 model prior to placement of low-infiltration covers.

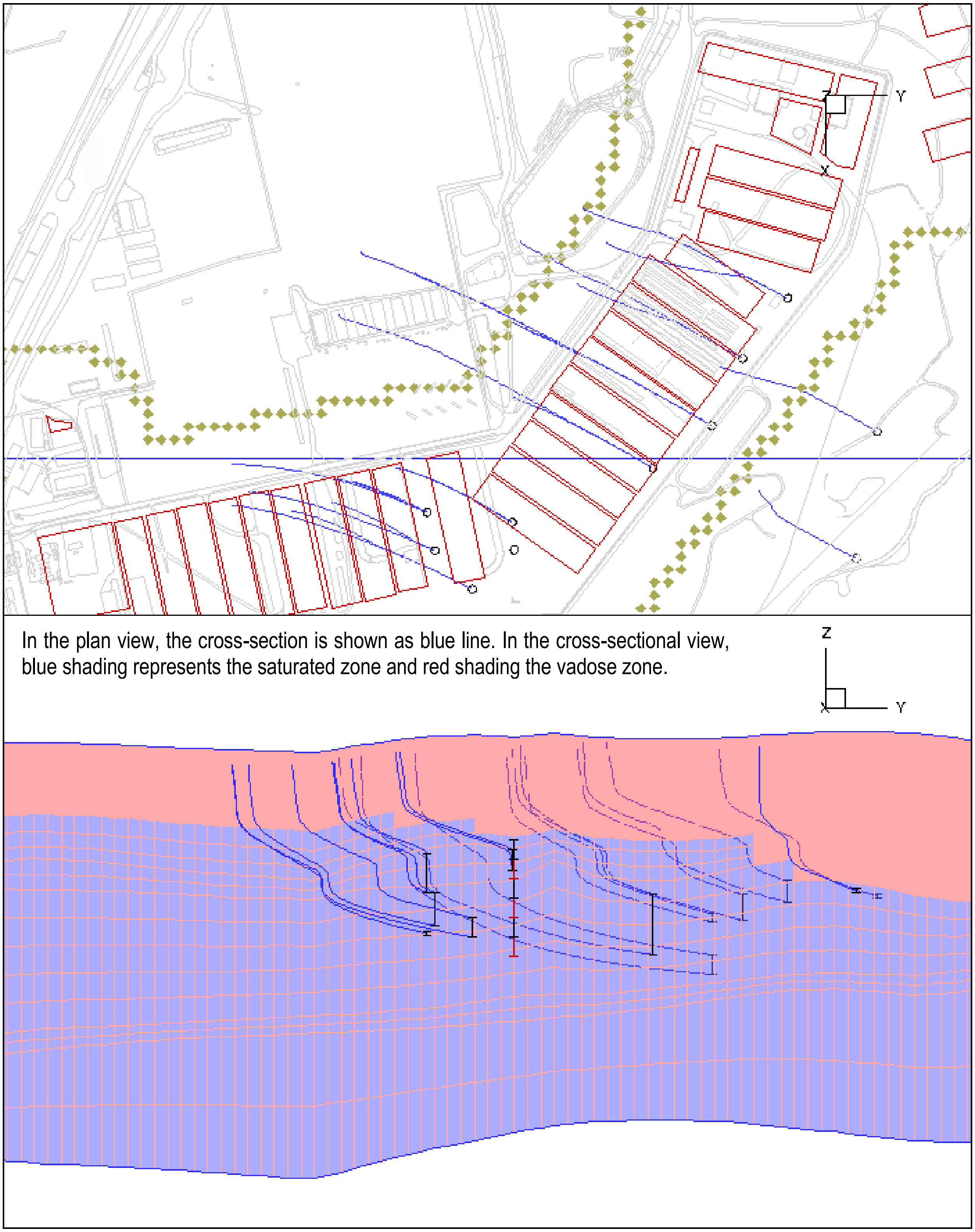

Figure 3-3. Simulated groundwater pathlines for GSA_2016 model after placement of low-infiltration covers.

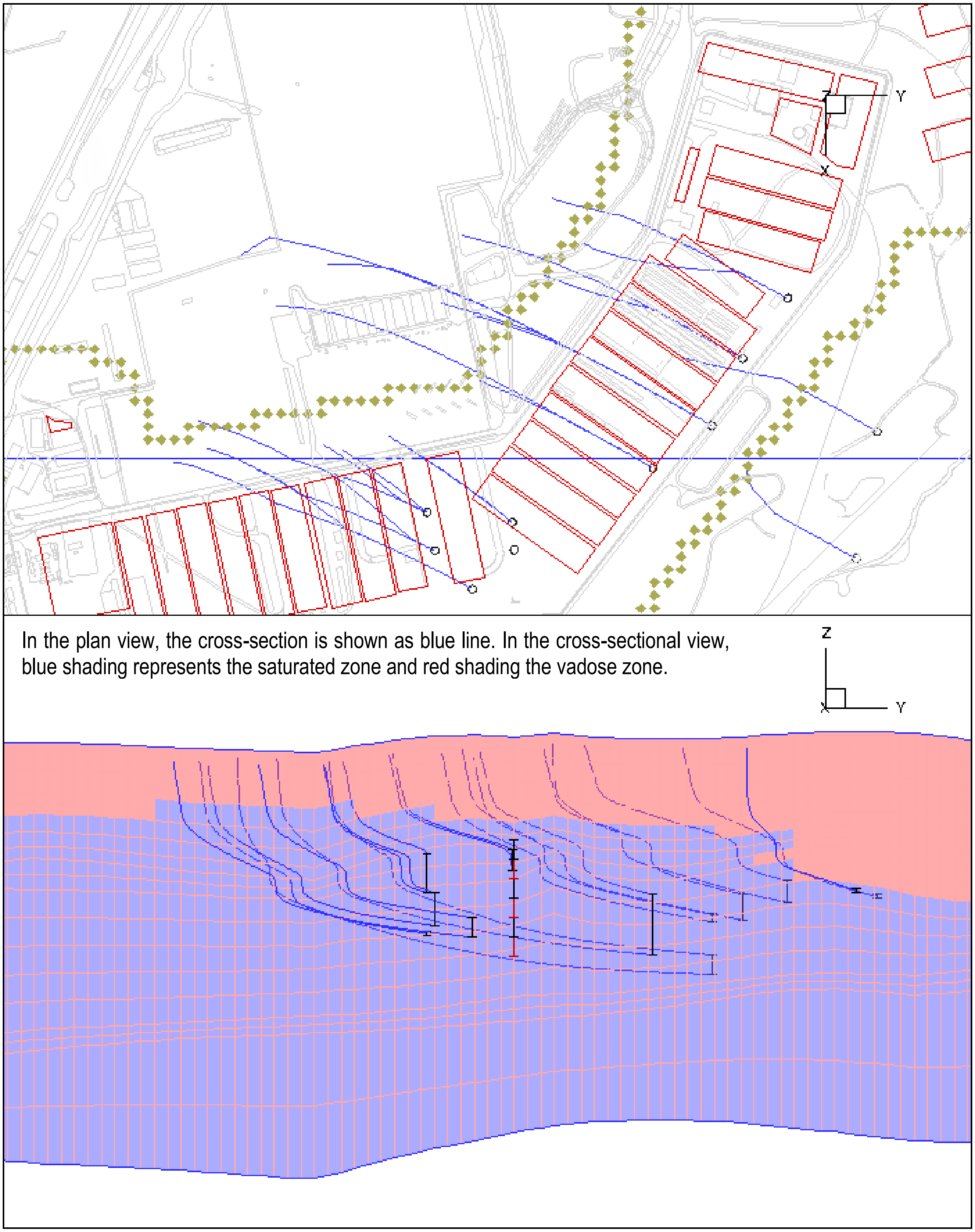

Figure 3-4. Simulated groundwater pathlines for GSA_2018 model prior to placement of low-infiltration covers.

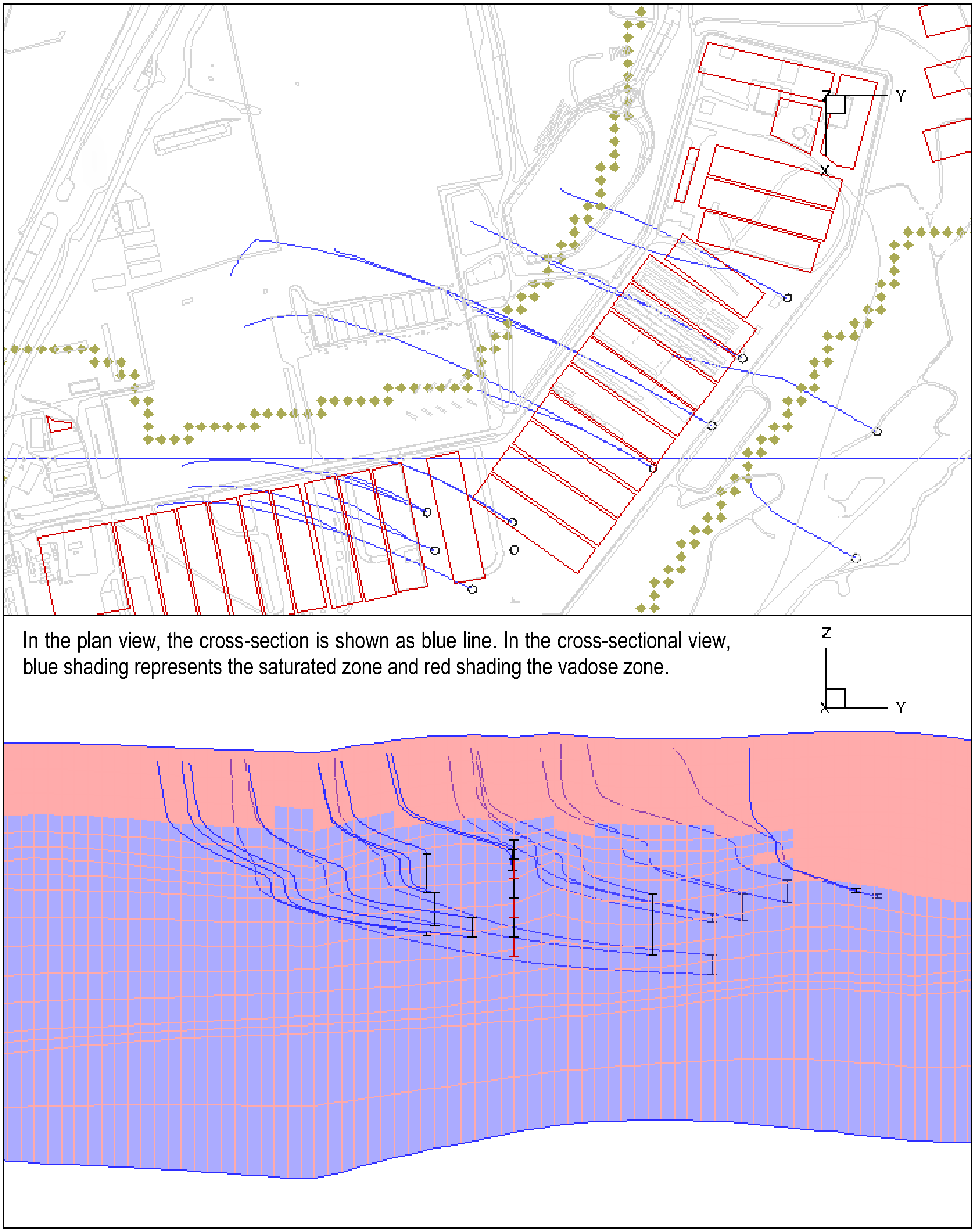

Figure 3-5. Simulated groundwater pathlines for GSA_2018 model after placement of low-infiltration covers.

4.0 Groundwater flow simulation results

This section presents simulation results for GSA_2018.LW (Layer-cake K field, Weighted targets), comparable to those presented in Sections 6 and 7 of Flach et al. (2017b) for the GSA_2016.LW = PEST.51 model.

4.1 PEST calibration

Table 4-1 summarizes the level of agreement between simulated and measured hydraulic heads for PEST optimization run 102 (PEST.102) corresponding to GSA_2018.LW. Compared to Flach et al. (2017b, Table 6-34, PEST.51), the GSA_2018.LW model exhibits a higher root-mean-square residual for the Gordon aquifer unit, similar r.m.s. head difference for the LAZ, and slightly lower r.m.s. residual in the UAZ. Stream baseflows for GSA_2018.LW (Table 4-2) are larger than GSA_2016.LW (Flach et al. 2017b, Table 6-35) because GCU leakance is lower causing higher groundwater discharges to nearby streams.

Table 4-1. Hydraulic head residual statistics.

HSU	Number	Median	Average	Root-mean-square	Minimum	Maximum
GAU	80	-1.1743	-1.6126	2.6939	-8.3457	2.7495
LAZ	285	1.9143	1.4866	5.2524	-15.2519	15.9644
UAZ	334	-0.1907	-0.1204	3.4494	-12.3604	13.5146

Table 4-2. Stream baseflow validation targets.

Parameter	Target	PEST.102
Average recharge (in/yr)†	N/A	12.1
Stream baseflow (ft^3/s)		
Upper Three Runs and tributaries excluding McQueen Branch	18.2	10.7
Fourmile Branch and tributaries	2.6	3.0
McQueen Branch	1.5	1.8
Crouch Branch	1.8	1.4

† Surface infiltration divided by total surface area including seepage faces.

Figure 4-1 shows individual hydraulic head residuals for the three aquifer zones, and the simulated water table. Table 4-3 summarizes the calibrated conductivity field. Compare these results to Figure 6-30 and Table 6-31 in Flach et al. (2017b).

In the GSA_2016.LW model, calibrated horizontal conductivity of the transmissive zone (TZ) within the Z-Area calibration polygon is 4.9 ft/d compared to 13.0 ft/d in the Global TZ region, and 8.1 ft/d in the Lower aquifer zone (LAZ) within the Z-Area polygon (Flach et al. 2017b, Table 6-31). This PEST optimization outcome does not agree with the general conceptual model of the TZ having a higher hydraulic conductivity than other aquifer zones within the Upper Three Runs aquifer. In the present GSA_2018.LW model, the horizontal conductivity of the TZ in Z-Area is 14.8 ft/d, identical to that in the Global TZ zone, and higher than LAZ conductivity. Thus, the GSA_2018.LW model recalibration to updated targets and using GCU K_v = 1.0e-5 ft/d improved agreement with the hydrogeologic conceptual model in Z-Area.

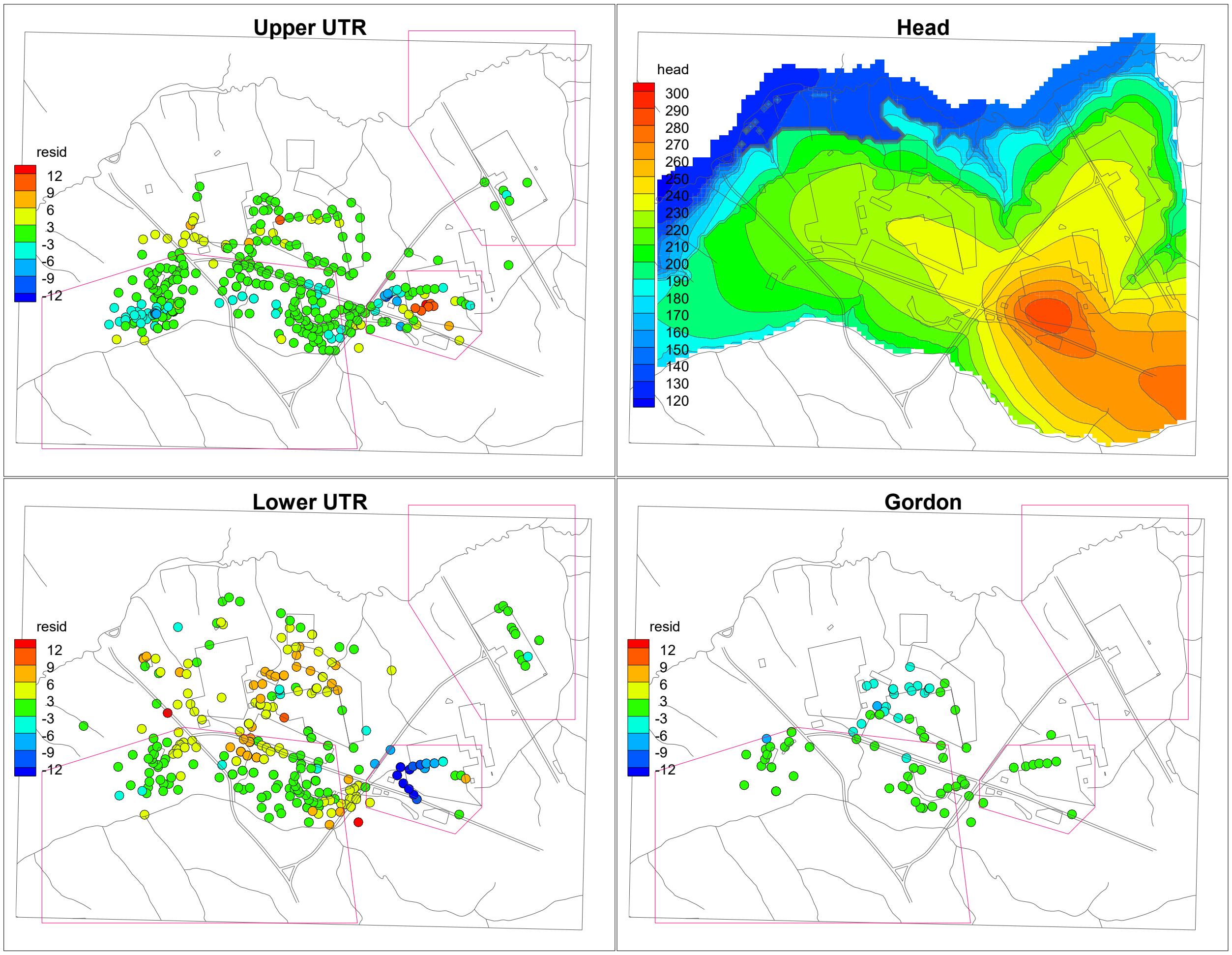

Figure 4-1. Hydraulic head residuals and water table surface for the GSA_2018.LW model.

Table 4-3. Hydraulic conductivity summary for the GSA_2018.LW model.

Parameter	Unit	Region	Base Kh (ft/d)	Base Kv (ft/d)	PEST.102c	Net Kh (ft/d)	Net Kv (ft/d)	Kh (cm/s)	Kv (cm/s)	Kh avg (ft/d)	Kv avg (ft/d)	log10 Kv	Kh,v ratio
Phi					79713								
N/A	GAU	Global	38	0.38									
N/A	GCU	Global	1.e-4	1.0e-5									
g01	LAZ	Global	8	0.267	1.18752	9.5	0.3	3.4E-03	1.1E-04	**7.2**	0.220	-6.58E-01	33x
g02	TCCZ	Global	0.18	0.006	0.444638	0.08	0.003	2.8E-05	9.4E-07	1.63E-01	**0.004**	-2.38E+00	39x
g03	TZ	Global	16	0.533	0.927212	14.8	0.49	5.2E-03	1.7E-04	**15.9**	0.513	-2.90E-01	31x
g04	AAA	Global	1	0.033	2.06358	2.06	0.068	7.3E-04	2.4E-05	**2.8**	0.123	-9.09E-01	23x
h01	LAZ	Harea			0.621258	5.9	0.2	2.1E-03	6.9E-05				
h02	TCCZ	Harea			0.01226666	0.001	3.3E-05	3.5E-07	1.2E-08				
h03	TZ	Harea			0.01453753	0.2	0.01	7.6E-05	2.5E-06				
h04	AAA	Harea			0.10151	0.21	0.007	7.4E-05	2.4E-06				
i01	LAZ	Zarea			0.572989	5.4	0.2	1.9E-03	6.4E-05				
i02	TCCZ	Zarea			0.744731	0.06	0.002	2.1E-05	7.0E-07				
i03	TZ	Zarea			0.994785	14.8	0.49	5.2E-03	1.7E-04				
i04	AAA	Zarea			2	4.13	0.136	1.5E-03	4.8E-05				
j01	LAZ	FHbasins			0.3	2.9	0.1	1.0E-03	3.4E-05				
j02	TCCZ	FHbasins			5	0.40	0.013	1.4E-04	4.7E-06				
j03	TZ	FHbasins			1.45352	21.6	0.72	7.6E-03	2.5E-04				
j04	AAA	FHbasins			2	4.13	0.136	1.5E-03	4.8E-05				

Simulation validation

Table 4-4 through Table 4-6 demonstrate that the GSA_2018.LW model conserves mass. In these tables, "IN" denotes the flowrate into the model, "OUT" the flowrate out of the model, and "NET" is their difference.

Table 4-4 lists flowrates across the six faces of the overall model domain. Total inflow and outflow differ by only 0.22%.

Table 4-5 presents mass balance results for each aquifer unit and zone, where GAU = Gordon aquifer unit, UTR = Upper Three Runs aquifer unit, UAZ = Upper aquifer zone within the UTR aquifer unit, and LAZ = Lower aquifer zone within the UTR aquifer unit. Again, inflows and outflows are observed to differ by a negligible amount, less than 0.3%.

Table 4-6 presents a global mass balance analogous to Table 4-4, but broken out by boundary condition type, where RECH## = recharge zone ##, GENH## = general head zone ##, and HEAD## = prescribed head zone ##. As expected from Table 4-4, the global mass discrepancy is shown as 0.22%.

Table 4-4. Global mass balance (ft^3/s).

BOUNDARY:	IN	OUT	NET FLOW	
ALL x-	1.303E-01	7.407E-01	-6.104E-01	
ALL x+	2.231E+00	0.000E+00	2.231E+00	
ALL y-	1.975E+00	0.000E+00	1.975E+00	
ALL y+	0.000E+00	1.777E-01	-1.777E-01	
ALL z-	3.030E-01	1.579E-02	2.872E-01	
ALL z+	1.002E+01	1.376E+01	-3.737E+00	
TOTALS	1.466E+01	1.470E+01	-3.201E-02	-0.22%

Table 4-5. Aquifer zone mass balances (ft^3/s).

BOUNDARY:	IN	OUT	NET FLOW	
GAU x-	1.053E-01	5.108E-01	-4.055E-01	
GAU x+	2.231E+00	0.000E+00	2.231E+00	
GAU y-	1.975E+00	0.000E+00	1.975E+00	
GAU y+	0.000E+00	1.777E-01	-1.777E-01	
GAU z-	3.030E-01	1.579E-02	2.872E-01	
GAU z+	4.681E-01	4.382E+00	-3.914E+00	
TOTALS	5.083E+00	5.087E+00	-4.031E-03	-0.08%

BOUNDARY:	IN	OUT	NET FLOW	
UTR x-	2.501E-02	2.298E-01	-2.048E-01	
UTR x+	0.000E+00	0.000E+00	0.000E+00	
UTR y-	0.000E+00	0.000E+00	0.000E+00	
UTR y+	0.000E+00	0.000E+00	0.000E+00	
UTR z-	8.196E-06	1.813E-01	-1.813E-01	
UTR z+	9.737E+00	9.379E+00	3.582E-01	
TOTALS	9.762E+00	9.790E+00	-2.798E-02	-0.29%

BOUNDARY:	IN	OUT	NET FLOW	
LAZ x-	2.467E-02	2.184E-01	-1.937E-01	
LAZ x+	0.000E+00	0.000E+00	0.000E+00	
LAZ y-	0.000E+00	0.000E+00	0.000E+00	
LAZ y+	0.000E+00	0.000E+00	0.000E+00	
LAZ z-	8.196E-06	1.813E-01	-1.813E-01	
LAZ z+	6.323E+00	5.964E+00	3.591E-01	
TOTALS	6.348E+00	6.364E+00	-1.588E-02	-0.25%

BOUNDARY:	IN	OUT	NET FLOW	
UAZ x-	3.332E-04	1.148E-02	-1.114E-02	
UAZ x+	0.000E+00	0.000E+00	0.000E+00	
UAZ y-	0.000E+00	0.000E+00	0.000E+00	
UAZ y+	0.000E+00	0.000E+00	0.000E+00	
UAZ z-	4.487E-01	5.622E+00	-5.174E+00	
UAZ z+	9.036E+00	3.863E+00	5.173E+00	
TOTALS	9.485E+00	9.497E+00	-1.210E-02	-0.13%

Table 4-6. Boundary condition mass balances (ft^3/s).

BOUNDARY:	IN	OUT	NET FLOW	IN	OUT	NET FLUX
RECH01:	9.852E+00	1.376E+01	-3.909E+00	1.204E+01	1.682E+01	-4.778E+00
RECH02:	1.124E-01	0.000E+00	1.124E-01	1.498E+01	0.000E+00	1.498E+01
RECH03:	1.678E-02	0.000E+00	1.678E-02	1.498E+00	0.000E+00	1.498E+00
GENH01:	2.544E-01	1.299E-02	2.414E-01	3.060E-01	1.563E-02	2.903E-01
GENH02:	2.164E-02	0.000E+00	2.164E-02	2.047E+02	0.000E+00	2.047E+02
GENH04:	2.030E-02	0.000E+00	2.030E-02	3.842E+01	0.000E+00	3.842E+01
HEAD01:	2.501E-02	2.298E-01	-2.048E-01	3.088E+01	2.838E+02	-2.529E+02
HEAD02:	4.360E+00	6.914E-01	3.669E+00	2.556E+02	4.053E+01	2.151E+02
TOTALS:	1.466E+01	1.470E+01	-3.237E-02	-0.22%		

Figure 4-2 compares simulated seepage faces (blue shading) to surveyed seeplines (white lines). Figure 4-3 compares simulated hydraulic heads to measured well water levels in the form of cross plots. See Figures 7-2 and 7-14 in Flach et al. (2017b) for comparable GSA_2016.LW results.

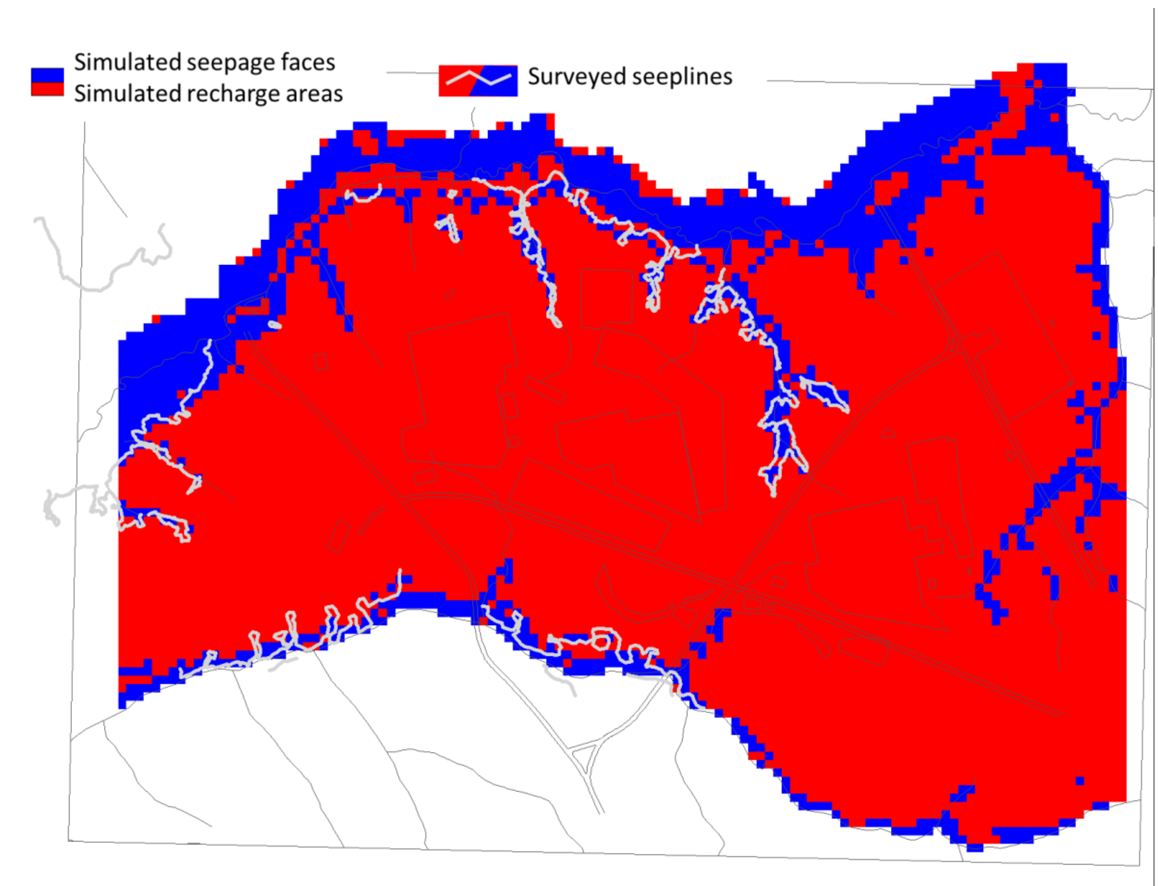

Figure 4-2. Simulated seepage faces compared to surveyed seeplines.

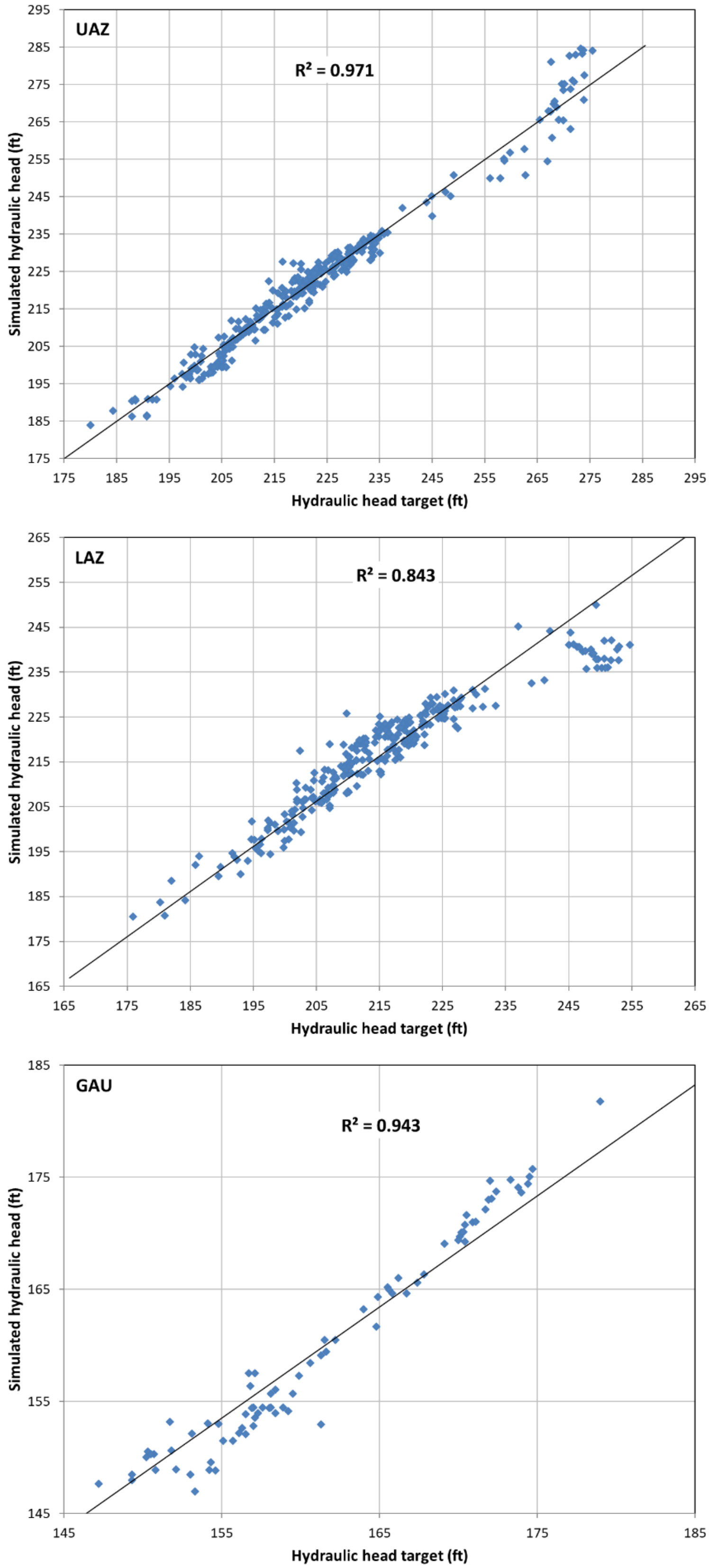

Figure 4-3. Hydraulic head crossplots.

4.2 Simulation results

Figure 4-4 through Figure 4-10 display simulated hydraulic heads, measured hydraulic heads, and simulated ground surface fluxes (recharge). The corresponding figures for GSA_2016.LW are found in Section 7.2 of Flach et al. (2017b).

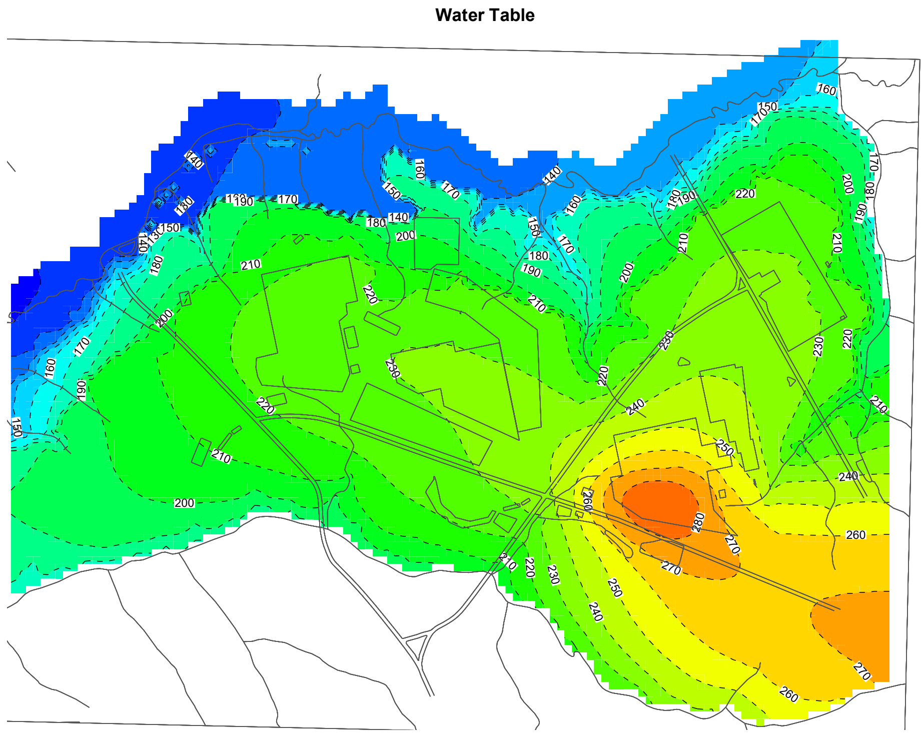

Figure 4-4. Simulated water table (ft).

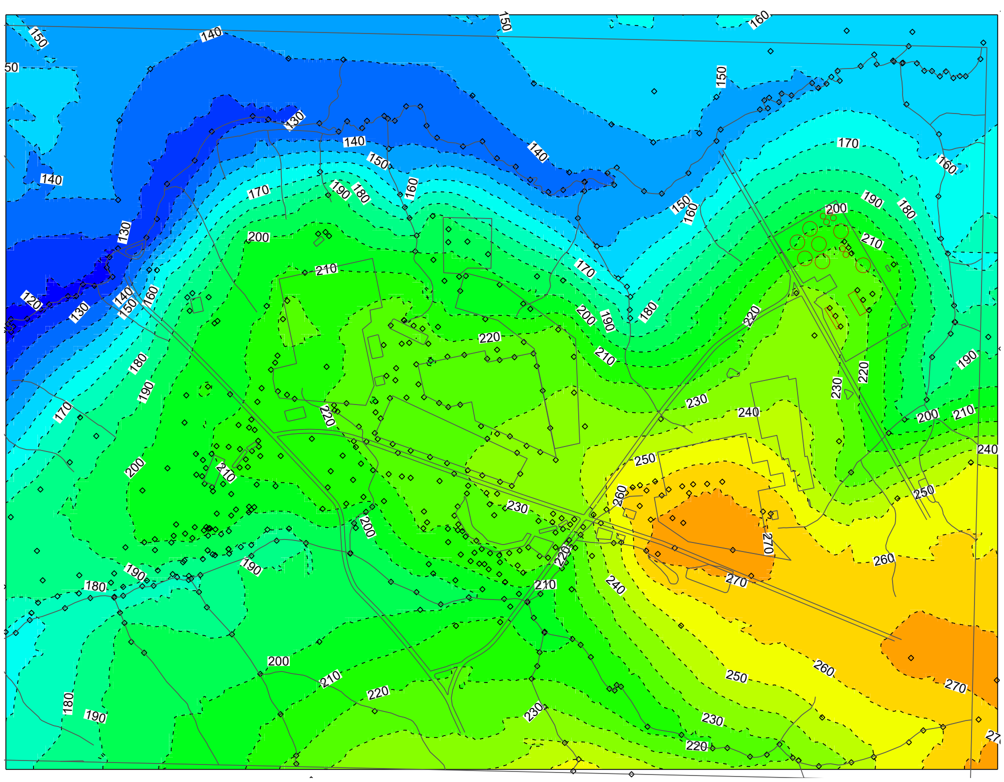

Key: open diamonds = data; solid diamonds = control points

Figure 4-5. Kriging interpolation representation of water table measurements (ft).

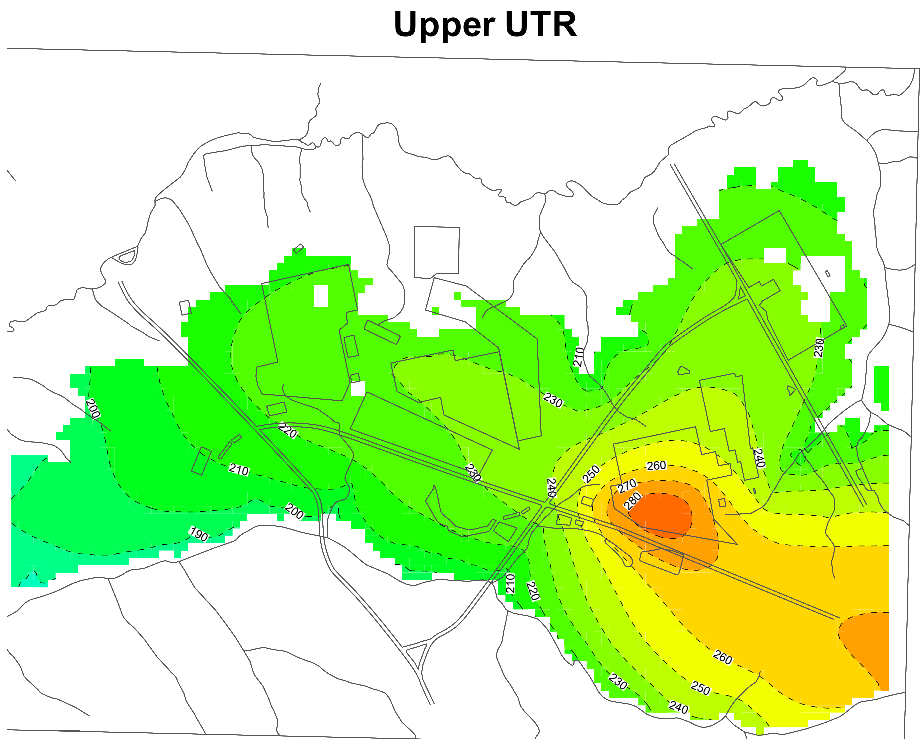

Figure 4-6. Simulated hydraulic head in the Upper Aquifer Zone (ft).

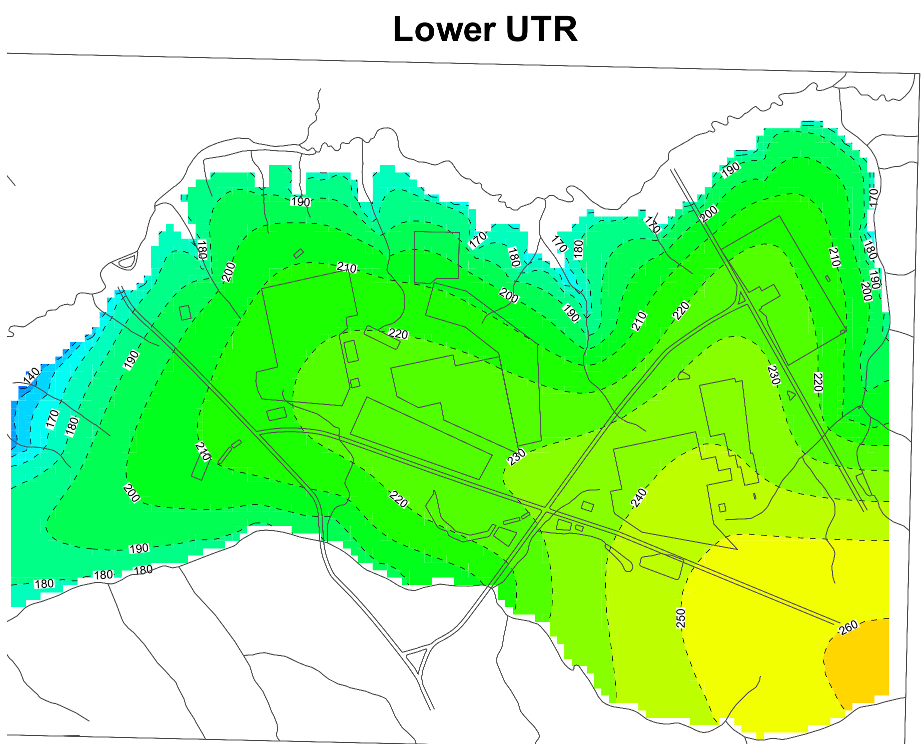

Figure 4-7. Simulated hydraulic head in the Lower Aquifer Zone (ft).

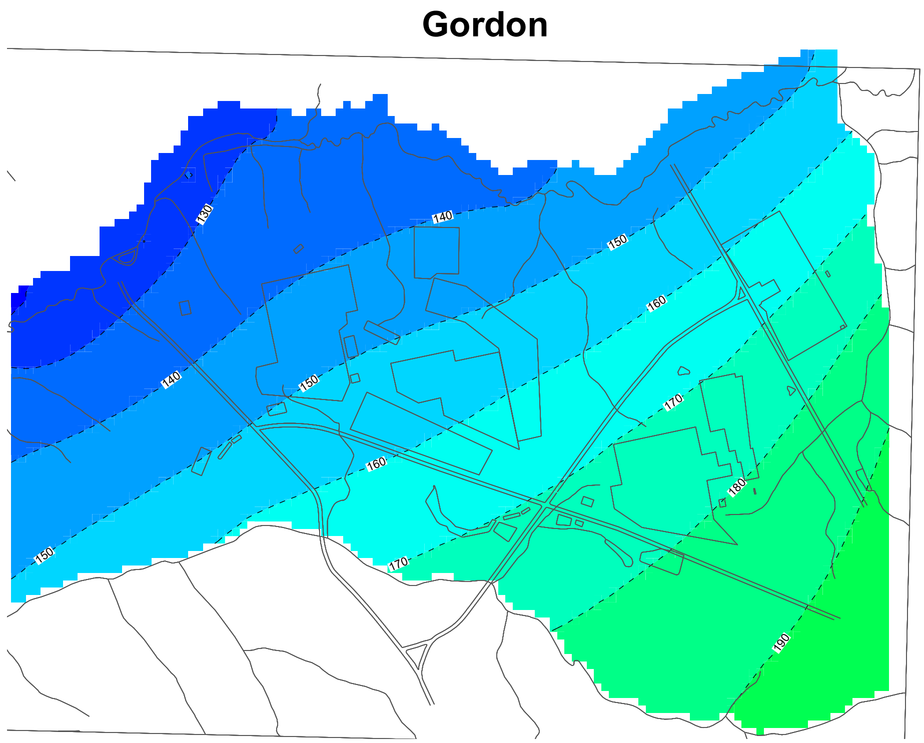

Figure 4-8. Simulated hydraulic head in the Gordon Aquifer Unit (ft).

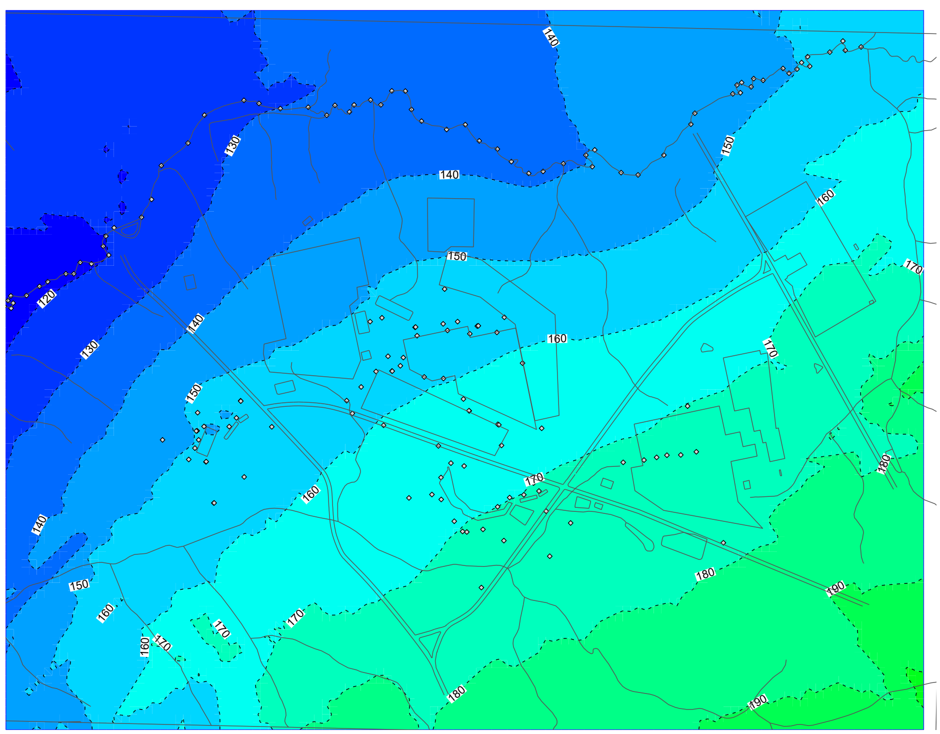

Figure 4-9. Kriging interpolation representation of Gordon aquifer unit (GAU) measurements (ft).

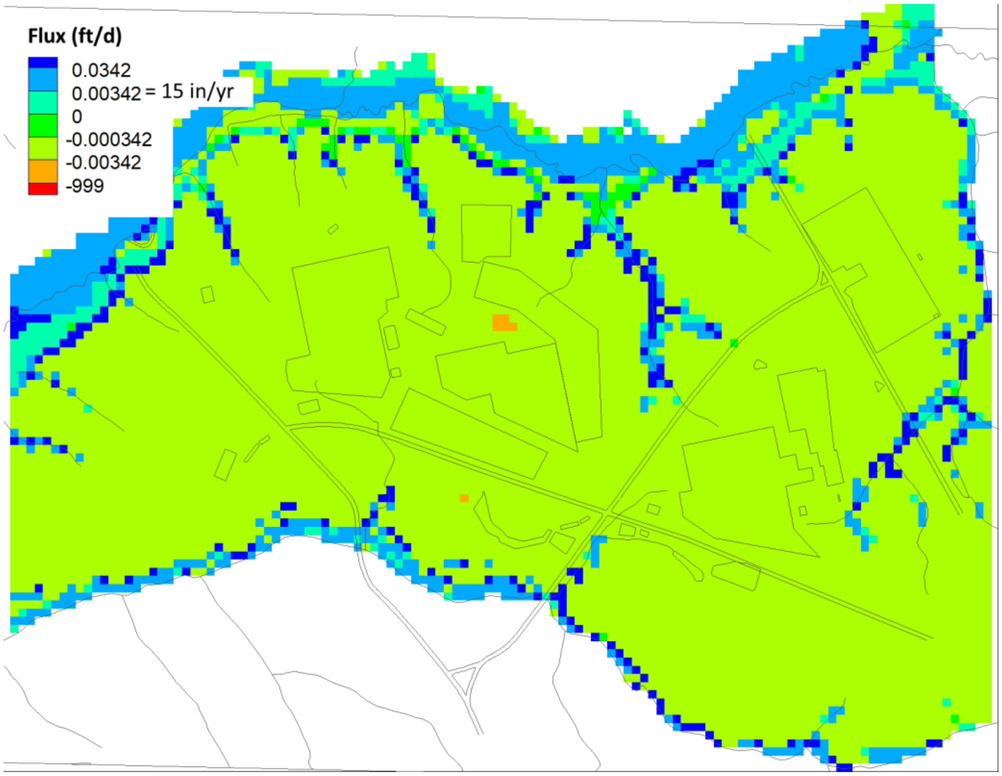

Note: negative values denote recharge, positive values discharge

Figure 4-10. Simulated surface flux (ft/d).

4.3 Simulation uncertainty

The parameter 95% confidence limits for GSA_2018.LW in Table 4-7 can be compared to Table 7-9 in Flach et al. (2017b).

Table 4-7. Parameter confidence limits.

Parameter description	Parameter ID	Estimated value	95% percent confidence limits	
			lower limit	upper limit
Global multiplier to LAZ	g01	1.18752	1.09265	1.29063
Global multiplier to TCCZ	g02	0.444638	0.376461	0.525161
Global multiplier to TZ	g03	0.927212	0.714795	1.20275
Global multiplier to AAA	g04	2.06358	0.637252	6.68235
HS-Area multiplier to LAZ	h01	0.621258	0.191975	2.01048
HS-Area multiplier to TCCZ	h02	1.226666E-02	1.458471E-04	1.03170
HS-Area multiplier to TZ	h03	1.453753E-02	5.662121E-06	37.3252
HS-Area multiplier to AAA	h04	0.101510	7.833978E-07	13153.3
Z-Area multiplier to LAZ	i01	0.572989	0.409960	0.800849
Z-Area multiplier to TCCZ	i02	0.744731	0.270276	2.05206
Z-Area multiplier to TZ	i03	0.994785	0.231014	4.28370
Z-Area multiplier to AAA	i04	2.00000	1.314937E-02	304.197
FH-Basins multiplier to LAZ	j01	0.300000	0.120565	0.746483
FH-Basins multiplier to TCCZ	j02	5.00000	2.35770	10.6035
FH-Basins multiplier to TZ	j03	1.45352	0.906665	2.33023
FH-Basins multiplier to AAA	j04	2.00000	0.299779	13.3431

4.4 Comparisons to GSA_2016 model

Figure 4-11 shows simulated groundwater pathlines for the GSA_2016.LW model, and Figure 4-12 shows pathlines for GSA_2018.LW. Kinks in the simulated pathlines (abrupt changes in direction) typically correspond to passage through the Gordon confining unit, where the groundwater flow direction differs from the overlying Lower aquifer zone.

Because the GCU hydraulic conductivity is lower for GSA_2018.LW (1.0e-5 versus 7.5e-5 ft/d), groundwater leakage into the Gordon aquifer unit is lower and groundwater travel is shallower. Fewer pathlines exhibit kinks, and pathlines tend to discharge at the ground surface sooner.

Figure 4-13 and Figure 4-14 reproduced from Flach (2017) show 1Q17 Tc-99 concentrations from sampling wells, and simulated groundwater pathlines based on the GSA_2016.LW model, respectively. Elevated Tc-99 detected at well ZBG-2 is thought to have originated from Cell G of SDU 4. Figure 4-15 compares backward groundwater particle tracks from the center of the ZBG-2 screen zone for the GSA_2016.LW and GSA_2018.LW flow models. Like Figure 4-11 and Figure 4-12, simulated groundwater flow in the GSA_2018.LW model is seen to travel on a more shallow trajectory than in the GSA_2016.LW model, which is expected considering the lower GCU hydraulic conductivity for GSA_2018.LW (1.0e-5 versus 7.5e-5 ft/d).

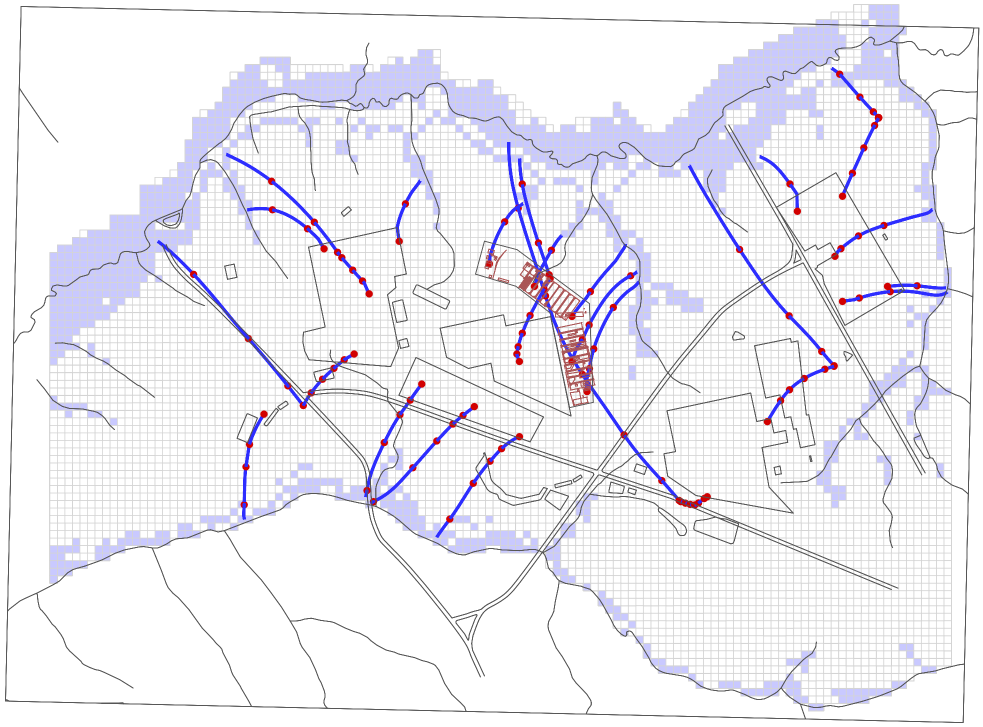

Figure 4-11. Particle tracking results for GSA2016.LW model.

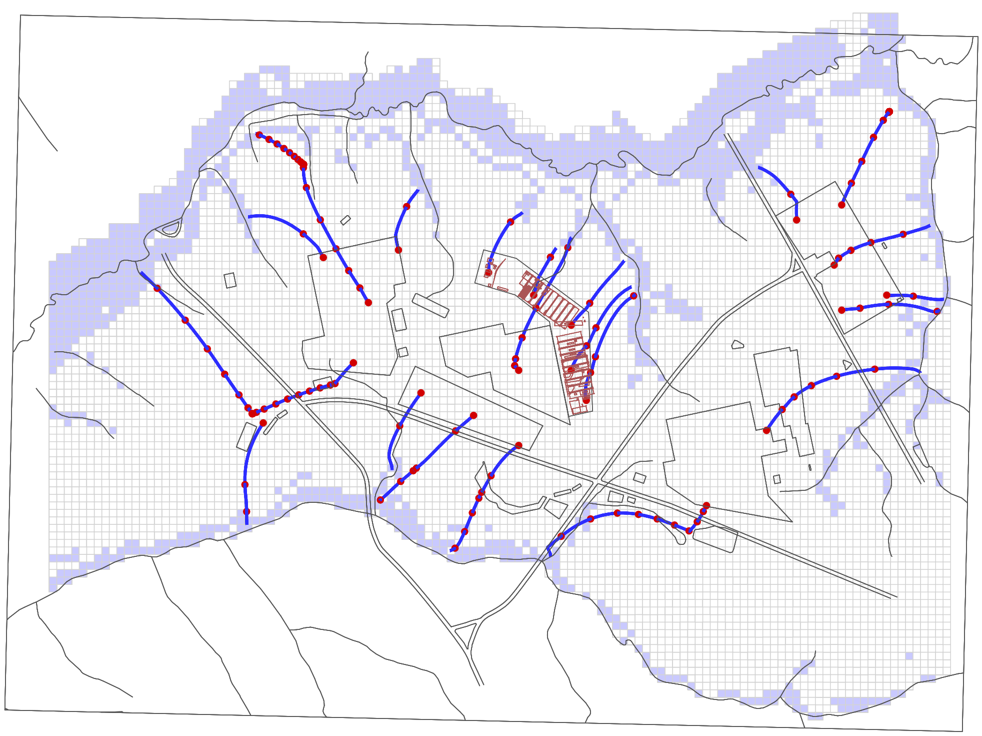

Figure 4-12. Particle tracking results for GSA2018.LW model.

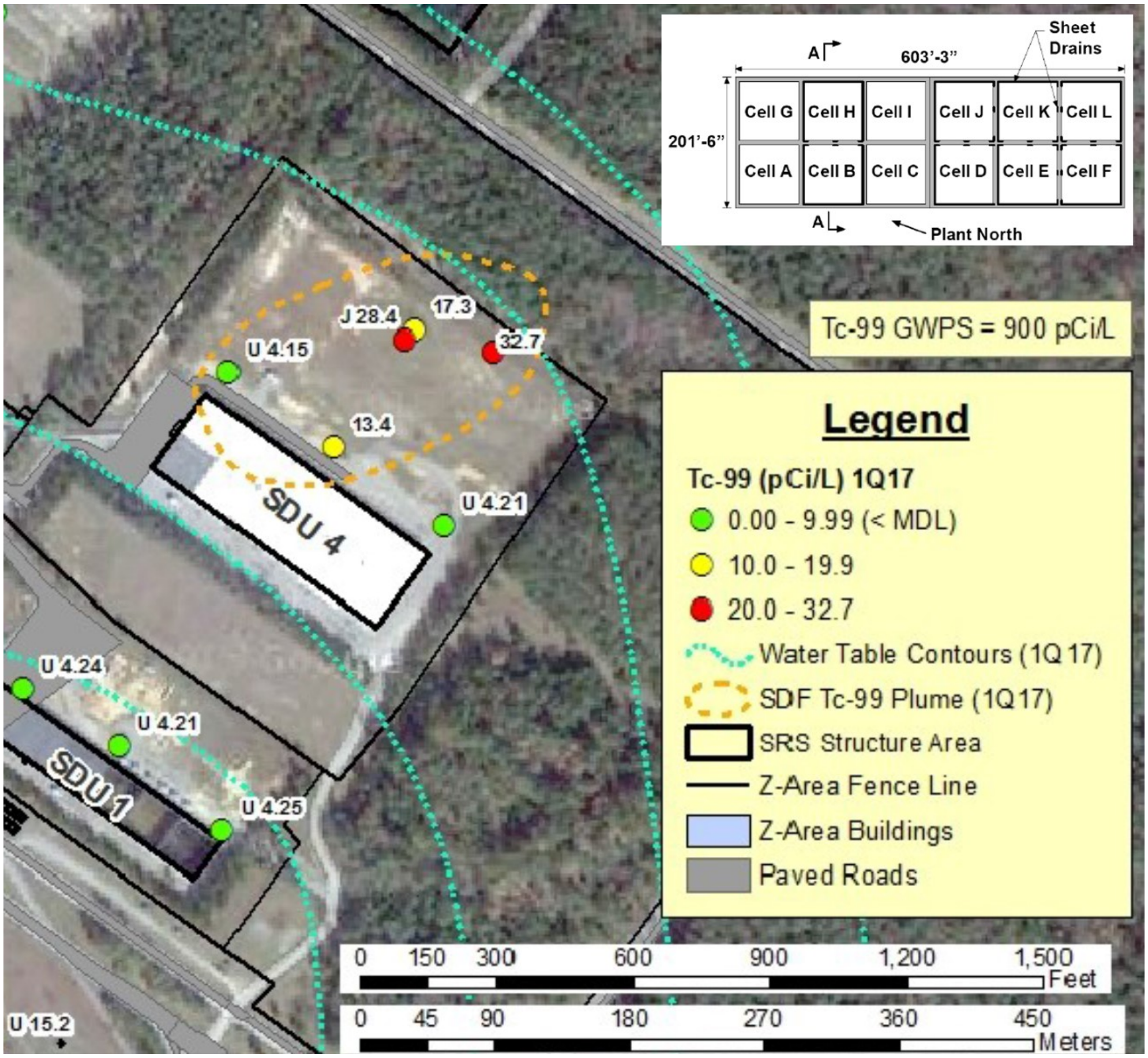

Figure reproduced from SRNL-L3200-2017-00107; modified from SRNS-TR-2017-00227.

Figure 4-13. Plan view of 1Q17 Tc-99 plume near SDU4

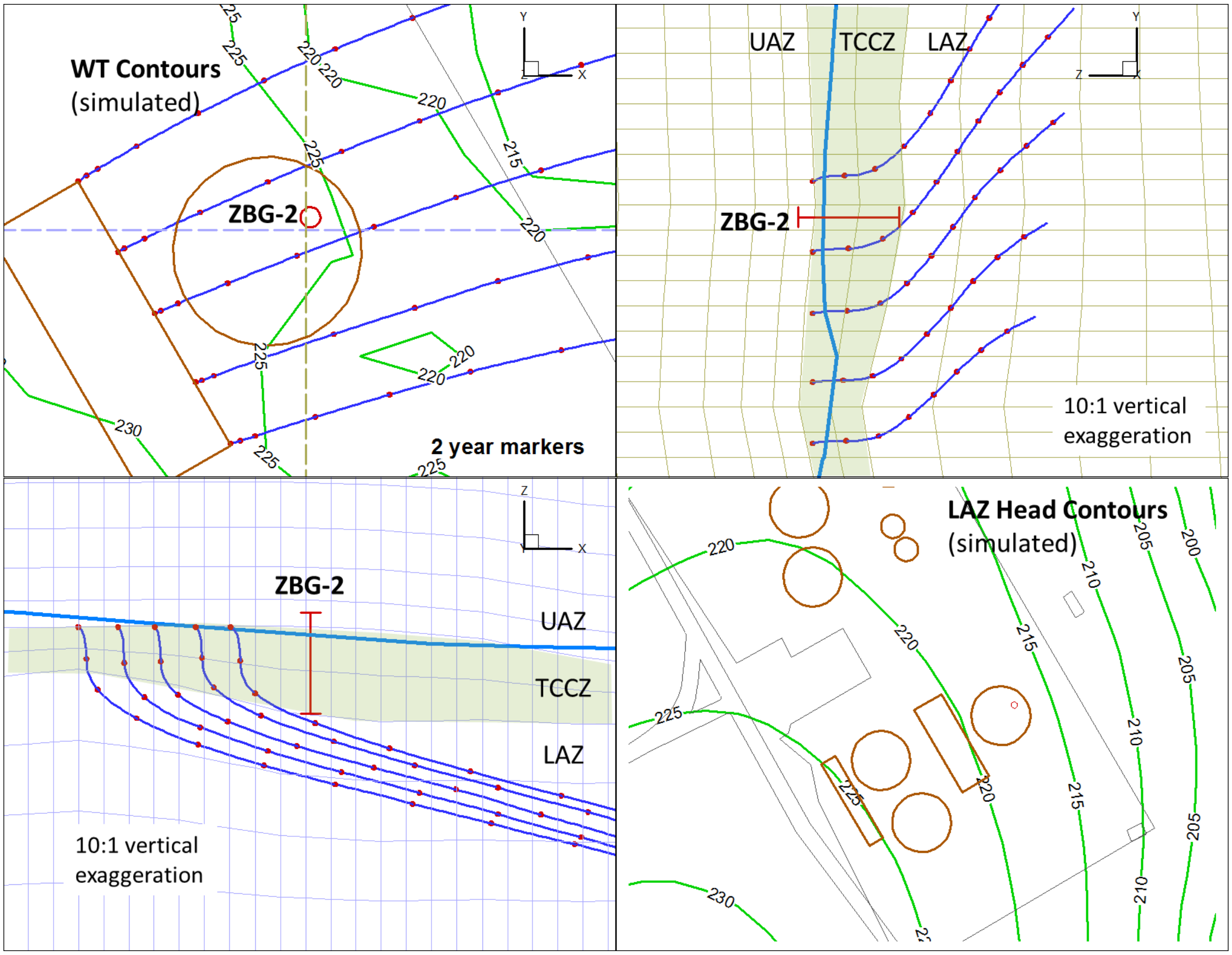

Figure reproduced from SRNL-L3200-2017-00107

Figure 4-14. Simulated groundwater particle tracks and head contours near Saltstone Disposal Unit 4 and well ZBG-2 based on the GSA_2016.LW model.

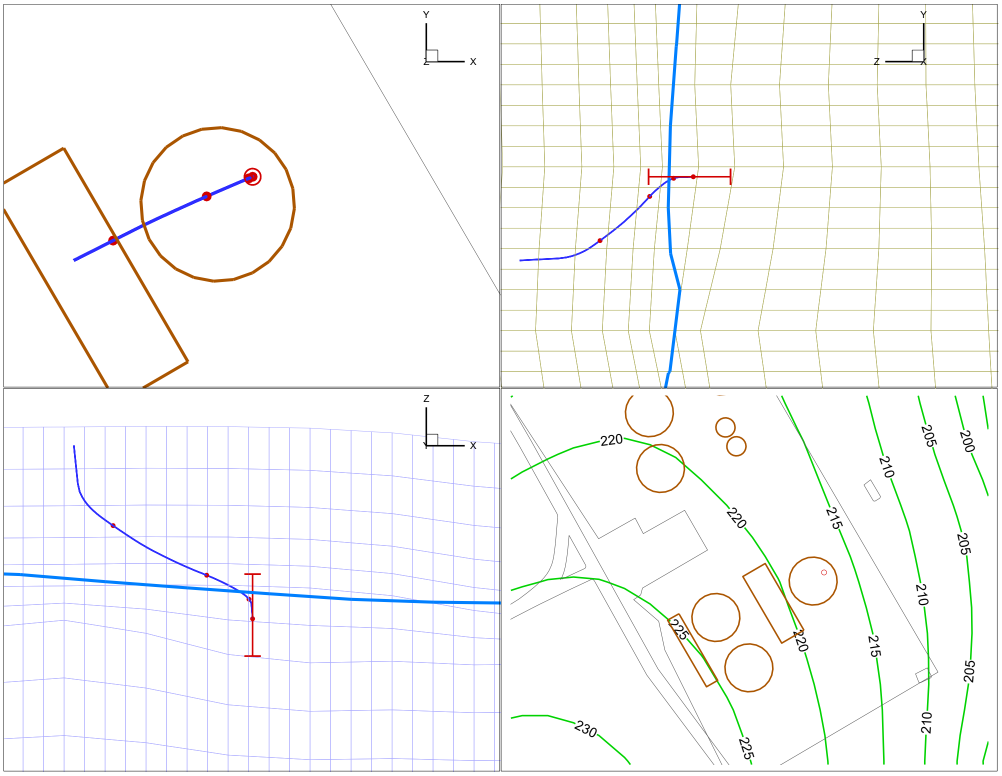

(a)

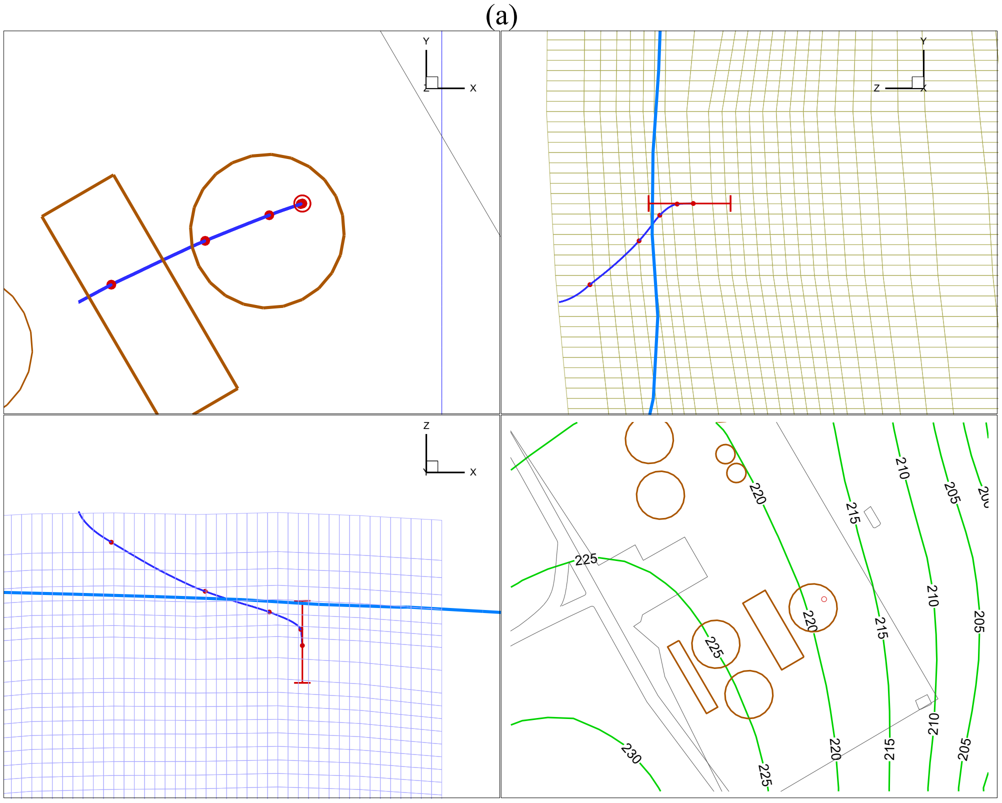

(b)

2-year time markers

Figure 4-15. Simulated groundwater pathlines near Saltstone Disposal Unit 4 and well ZBG-2 based on the (a) GSA_2016.LW, and (b) GSA_2018.LW models.

5.0 References

Bagwell, L. A., P. L. Bennett and G. P. Flach. *General Separations Area (GSA) Groundwater Flow Model Update: Hydrostratigraphic Data*. SRNL-STI-2016-00516 Revision 0. February 2017.

Flach, G. P. *Code Selection for General Separations Area Flow Simulation and Model Calibration*. SRNL-TR-2015-00061, Revision 0. March 2015.

Flach, G. P. *Groundwater particle tracking and tracer transport simulations near Saltstone Disposal Unit 4 and Well ZBG-2*. SRNL-L3200-2017-00107. September 2017.

Flach, G. P., L. A. Bagwell and P. L. Bennett. *Groundwater Flow Simulation of the Savannah River Site General Separations Area*. SRNL-STI-2017-00008 Revision 0. May 2017a.

Flach, G. P., L. A. Bagwell and P. L. Bennett. *Groundwater Flow Simulation of the Savannah River Site General Separations Area*. SRNL-STI-2017-00008 Revision 1. September 2017b.

Hiergesell, R. A., Taylor, G. A., Phifer, M. A., Whiteside, T. S., and Flach, G. P. *General Separations Areas groundwater model calibration targets*. SRNL-STI-2015-00351 Revision 0. August 2015.

Kubilius, W. P. and W. D. Joyce. *Optimization of the Groundwater Monitoring Program at the E-Area Low-Level Waste Facility (ELLWF)*. SRNL-RP-2018-01123. December 2018.

Wohlwend, J. L. *Updated General Separations Areas (GSA) Groundwater Model Calibration Targets*. SRNL-STI-2018-00336, Revision 0. July 2018.

Distribution:

timothy.brown@srnl.doe.gov
alex.cozzi@srnl.doe.gov
david.crowley@srnl.doe.gov
david.dooley@srnl.doe.gov
a.fellinger@srnl.doe.gov
samuel.fink@srnl.doe.gov
nancy.halverson@srnl.doe.gov
erich.hansen@srnl.doe.gov
connie.herman@srnl.doe.gov
david.herman@srnl.doe.gov
kevin.fox@srnl.doe.gov
john.mayer@srnl.doe.gov
daniel.mccabe@srnl.doe.gov
gregg.morgan@srnl.doe.gov
frank.pennebaker@srnl.doe.gov
william.ramsey@srnl.doe.gov
luke.reid@srnl.doe.gov
geoffrey.smoland@srnl.doe.gov
michael.stone@srnl.doe.gov
boyd.wiedenman@srnl.doe.gov
bill.wilmarth@srnl.doe.gov
Records Administration (EDWS)

sebastian.aleman@srnl.doe.gov
tom.butcher@srnl.doe.gov
tim.coffield@srs.gov
kerri.crawford@srs.gov
thomas.danielson@srnl.doe.gov
james.dyer@srnl.doe.gov
gregory.flach@srnl.doe.gov
luther.hamm@srnl.doe.gov
thong.hang@srnl.doe.gov
ginger.humphries@srs.gov
vijay.jain@srs.gov
daniel.kaplan@srnl.doe.gov
walt.kubilius@srnl.doe.gov
dien.li@srs.gov
larry.romanowski@srs.gov
kent.rosenberger@srs.gov
jansen.simmons@srs.gov
ira.stewart@srs.gov
kevin.tempel@srs.gov
steven.thomas@srs.gov
jennifer.wohlwend@srnl.doe.gov
tad.whiteside@srnl.doe.gov
peter.fairchild@srs.gov
paul.andrews@srs.gov
verne.mooneyhan@srs.gov